

# Compact Low-Cost Millimeter-Wave Radar Sensor for Short-Range Applications

Ignacio Sardinero-Meirás<sup>(1)</sup>, Elías Antolinos<sup>(1)</sup>, Ignacio E. López-Delgado<sup>(1)</sup>, Marcos Gómez-Bracamonte<sup>(1)</sup>, Jaime Fernández-Martínez<sup>(1)</sup>, Lorena Perez-Eijo<sup>(2)</sup>, Marcos Arias<sup>(2)</sup>, Borja Gonzalez-Valdes<sup>(2)</sup>, Jesús Grajal<sup>(1)</sup>

E-mail: i.sardinero@upm.es

<sup>(1)</sup>Information Processing and Telecommunications Center, Universidad Politécnica de Madrid, E.T.S.I Telecomunicación, Av. Complutense 30, 28040 Madrid, Spain.

<sup>(2)</sup>Atlantic Research Center, Universidade de Vigo, 36310 Vigo, Spain.

**Abstract**—A millimeter-wave radar for short range applications has been developed using COTS components. Radar performance, wireless operation and scalability in a radar network operation have been the main drivers. This device has been tested in structural health and vital sign monitoring scenarios.

**Index Terms**—radar, MMIC, millimeter-wave, structural health monitoring, vital signs

## I. INTRODUCTION

Several short-range monitoring applications require the following characteristics [1]–[4]:

- Remote sensing: the contact with the target may not be possible, or may affect the measurement.
- High accuracy to detect  $\mu\text{m}$  displacements.
- Day&Night detection: continuous monitoring regardless the light conditions in the environment.
- Privacy-preserving: the monitoring should be carried out without collecting sensitive data.
- Portable: the sensing devices must require low-power consumption and be interconnected wirelessly.
- Low-cost devices: sensors may be escalated to form networks, so the unitary price of the node must be low.

In this paper we present a multi-purpose radar which satisfies the aforementioned requirements, as there is no commercial radar known to the authors with these capabilities. The radar is a modified version of a 124 GHz FMCW commercial radar kit manufactured by Silicon Radar [5].

The performance of the radar has been tested in structural health and human health monitoring scenarios with very promising results. In structural health monitoring (SHM) scenarios the radar is capable of detecting the vibration of structures such as bridges and buildings with a  $\mu\text{m}$  precision. This information is crucial to prevent damages caused by critical structure health states.

In human health applications the radar is capable of continuously monitoring the vital signs of a person, analyzing the chest's displacement, in the  $\mu\text{m}$  range, due to the movement of the heart and lungs.

Section II describes the architecture of the designed system, highlighting the modifications carried out to the commercial device. Section III presents the results obtained in human health and structural health monitoring applications. Finally, conclusions are drawn in Section IV.

## II. ARCHITECTURE

The radar node is a modified version of the commercial 124 GHz FMCW radar kit developed by Silicon Radar, (see Fig. 1), developed to fulfill the application requirements. A photograph of the fully assembled system is shown in Fig. 2. The new version of the system preserves the commercial RF front-end from Silicon Radar, based in a TRA\_120\_045 Microwave Integrated Circuit (MMIC) [6]. The main modifications, which are detailed throughout this section and summarized in Table I, are implemented in three custom-made PCBs.

TABLE I: Comparison between the commercial and the modified versions

	Commercial version	Modified version
Operating mode	LFMCW	CW LFMCW
Continuous transmission	No	Yes
Wireless	WiFi 802.11b/g/n	Bluetooth 5.3
Sampling frequency	5 Msps	500 ksps*
Power consumption	> 5 W	2 W
Size	10x7 cm <sup>2</sup>	7.5x5 cm <sup>2</sup>
Cost	1000€	180€

\* A recently updated version of the microcontroller provides 1 Msps sampling frequency per channel [10].

### A. 3D-printed lens

The commercial kit used an acrylic focusing lens to reduce the antenna beamwidth to  $4^\circ$  in both planes. This lens was replicated in 3D-printing material (ABS). No differences were observed in the antenna beamwidth with the 3D-printed lens.

### B. Baseband board

The baseband board allocates a phase frequency detector to control the transmitted waveform and a signal conditioning stage, which amplifies and filters the IQ signals. Low pass filters are implemented to allow both CW and LFMCW operation modes, which was not possible in the commercial kit. Moreover, the gain of the amplifying stage has been reduced in order to optimize the power consumption of the radar node.

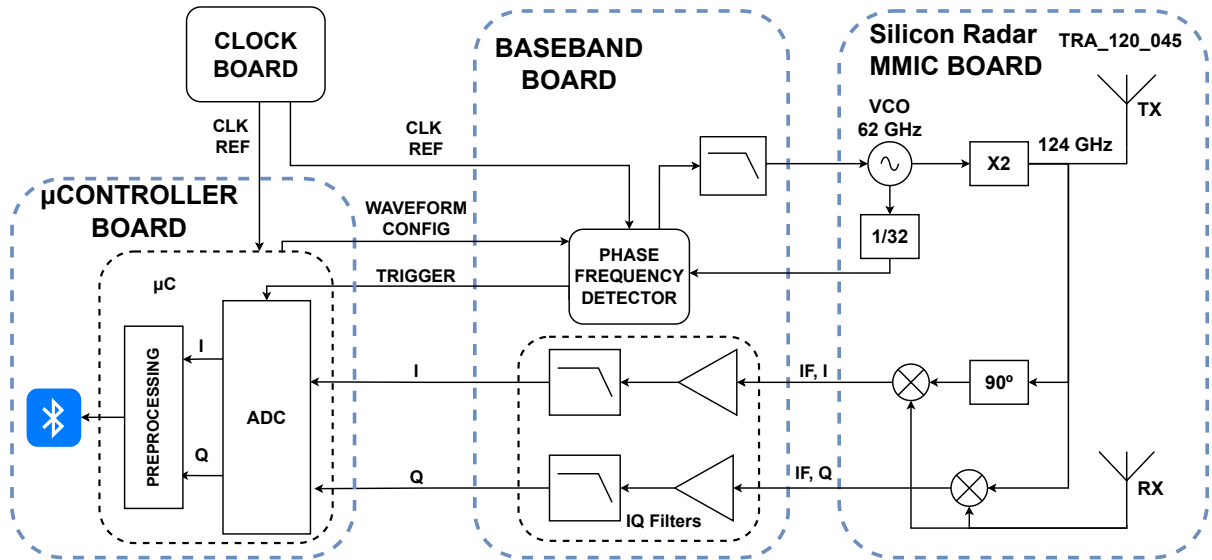


Fig. 1: Diagram of the radar node architecture. It shows from right to left: the commercial RF front-end, the baseband board, the clock board and the microcontroller board.

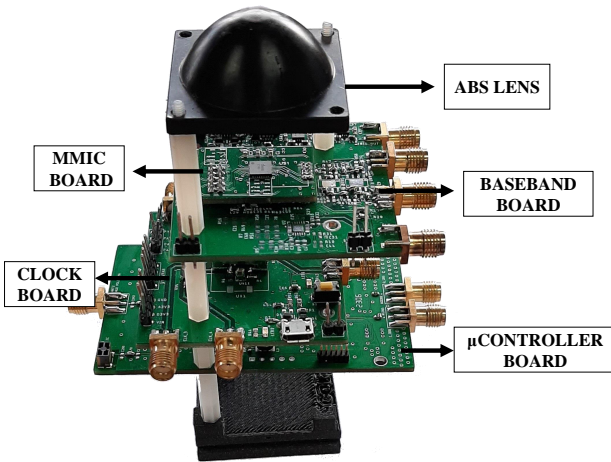


Fig. 2: Custom-made radar node. From bottom to top: the microcontroller board, the clock board, the baseband board, the MMIC board and the ABS lens.

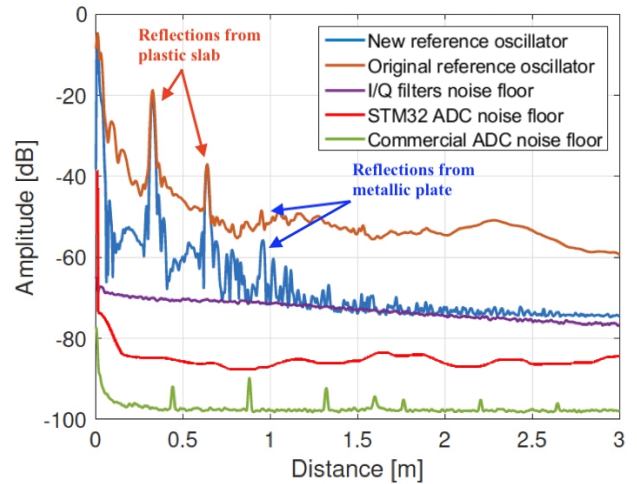


Fig. 3: Spectral noise floor comparison among different stages of the radar's architecture. The radar aims at two targets in its line of sight: a penetrable plastic slab and a metallic plate behind it.

### C. Clock board

The clock reference of the commercial kit was replaced with a commercial oscillator that provides less phase noise [8]. This is an important feature in an upconversion architecture, because the phase noise increases in each multiplication stage, ultimately masking close low-power targets in the spectrum. This effect is shown in Fig. 3 [9], where the reduction in the phase noise caused by the new reference oscillator allows the detection of the previously masked target at around 1 m distance. Therefore, the signal-to-noise ratio (SNR) is enhanced with respect to the commercial version.

The new reference oscillator was mounted in a separate module which allows the distribution of the clock signal for the synchronization of several nodes within the same radar network.

### D. Microcontroller board

The modified version uses the low-cost commercial microcontroller STM32WB15CC ( $\sim 6\text{€}$ ) [7]. This microcontroller has a 12-bit ADC with a maximum sampling frequency  $f_s = 1\text{ Msps}$ , i.e. it can sample the I and Q channels at  $f_s = 500\text{ kpsps}$  each. This sampling frequency is compatible with typical short-range configurations. For instance, ranges below 6.25 meters can be measured configuring the radar with a bandwidth  $B = 6\text{ GHz}$ , and a chirp time  $T_c = 1\text{ ms}$ . Notice that this configuration can be modified to measure different ranges.

The noise floors of the ADC of the microcontroller and a high-performance ADC ADLink 9846D ( $\sim 3600\text{€}$ ) are compared in Fig. 3. As it is shown, the noise level of the microcontroller is  $\sim 15\text{ dB}$  higher. Still, the SNR measured

with the modified radar suffices for the targeted applications.

The sampled data is preprocessed in the microcontroller to achieve real-time processing with continuous wireless transmission. This is not generally implemented in commercial systems because of the high data-rates generated. Commercial systems usually process one out of several interrogations [5]. This way, they achieve real-time processing by losing useful information. In the radar designed, only the FFT-bins where the target is contained are transmitted via Bluetooth to an external processing unit. This way, all the interrogations and all the target information is processed.

### E. Power consumption reduction

The Silicon-Radar commercial version needs two microcontrollers: one to sample the data, and another one to handle the wireless link. The microcontroller used in the modified version allows the implementation of the Bluetooth protocol on-chip by running two CPUs in parallel: the main CPU handles the data sampling and preprocessing, and the secondary CPU handles the Bluetooth stack protocol. Reducing the number of microcontrollers from two to one, reduces the power consumption of the system.

Moreover, the modifications carried out on the baseband board result into a power consumption reduction, as the signal conditioning stages of the baseband board are simplified. As a result, the modified version can be powered with a commercial low cost power bank with higher battery life.

## III. APPLICATIONS

This section presents the results obtained with the radar module in different applications. All the measurements presented are carried out using the same configuration: LFMCW mode, central frequency ( $f_c$ ) of 121 GHz, a transmitted bandwidth ( $B$ ) of 6 GHz and a sweep time ( $T_c$ ) of 1 ms.

### A. Structural Health Monitoring

Structural health monitoring (SHM) is a process used to assess and monitor the health and integrity of various infrastructures, such as bridges and buildings. The designed radar can sense  $\mu\text{m}$ -movements, and therefore it can be used for Vibration-Based SHM [11].

To characterize the accuracy of the system, a static target has been measured at different SNR levels. The results are shown in Fig. 4. The results are clearly close to Cramér-Rao Lower Bound (CRLB), computed with Eq. 1 [12]:

$$\text{var}(\hat{R}) \geq \left(\frac{c}{4\pi}\right)^2 \frac{1}{2 \text{SNR}} \frac{1}{N f_c^2 + B f_c (N-1) + \frac{B^2 (2N-1)(N-1)}{6N}} \quad (1)$$

where  $N$  is the signal length. Note that the SNR used is before applying the FFT. As expected, the standard deviation is inversely proportional to the SNR.

Once the radar accuracy has been characterized, a pillar supporting a bridge is monitored (setup shown in Fig. 5a). A person standing in the center of the bridge jumps at the instant  $t = 2$  s. The displacement measured with the radar and its spectrogram are shown in Fig. 5b. As it is observed, the maximum displacement of the pillar is  $17\mu\text{m}$ , and its resonance frequency is 21 Hz.

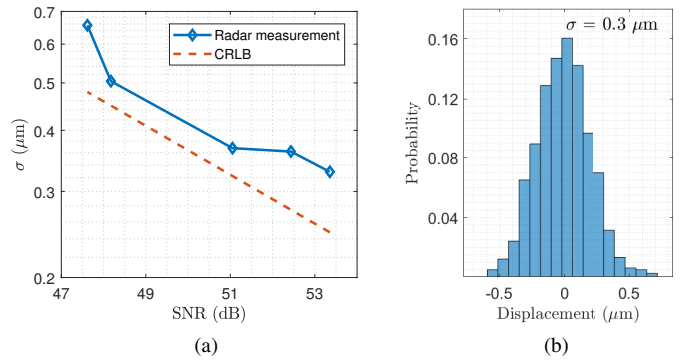


Fig. 4: Radar displacement accuracy obtained measuring a static target ranging between 0.2 and 1.2 meters. 1000 consecutive interrogations are analyzed for each range. (a) Radar displacement accuracy measured along the signal-to-noise ratio compared with the CRLB. (b) Histogram of the distance displacements due to phase shifts when SNR = 53.5 dB.

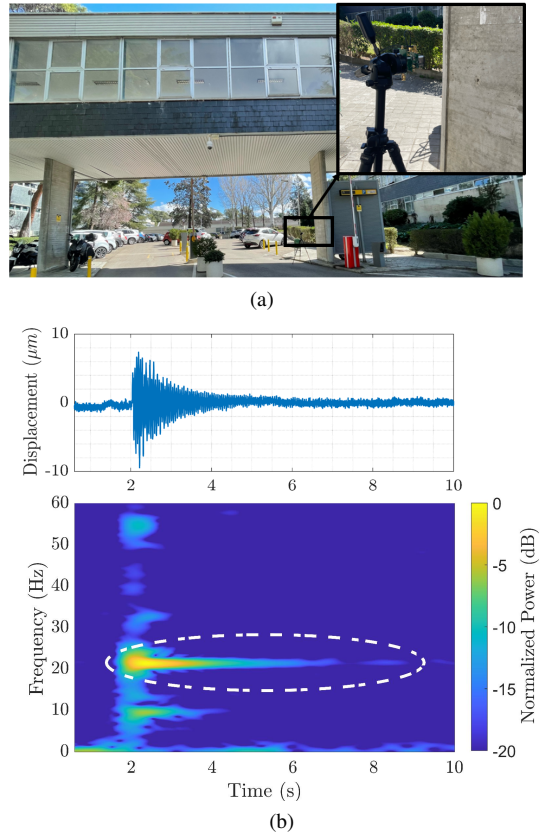


Fig. 5: Vibration-Based SHM with the designed radar node. (a) Radar setup pointing a pillar at 1 m. (b) Displacement obtained with the radar node (top), it shows a maximum variation of  $17\mu\text{m}$ , and spectrogram of the movement measured (bottom), where the resonance frequency can be clearly identified as 21 Hz.

### B. Human health monitoring

Non-contact human health monitoring has gained attraction in the past decade since it is a promising solution to overcome difficulties in some scenarios, such as sleep monitoring, or in the early detection of some diseases in telehealth or

home-monitoring scenarios. Human health monitoring can be approached from two different perspectives:

- Range monitoring, which focuses on the analysis of the cardiopulmonary activity using the displacement information that is contained in the phase of the radar signal acquired. Under this approach, it has been analyzed the chest's wall displacement due to the breathing and heart movement [13].
- Doppler monitoring, which focuses on analysing the micro-Doppler and range-time signatures of diverse body parts. For instance, it is possible to extract motor biomarkers from the micro-Doppler signature of the gait to detect diseases such as Parkinson's Disease [14].

Regarding to the cardiopulmonary activity analysis, a target which is sitting in front of the radar at 0.5 m has been measured. The obtained signals are represented in Fig. 6. Results show that the system is capable of monitoring the breathing and heartbeat of a person, being able to extract the HRV accurately. The processing to extract these waveforms is described in [13]. Fig. 6 also shows that we are capable of appreciating a well-known phenomenon called respiratory sinus arrhythmia, which consists of the heart pulse speeding up during inspiration (so the time interval between consecutive pulses, and therefore, the HRV sequence, decreases) and speeding down during exhalation.

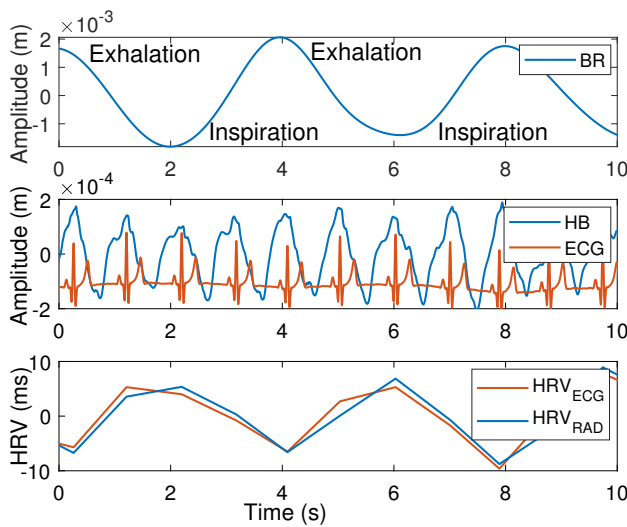


Fig. 6: Comparison between the signals obtained with the radar and the reference sensor. From top to bottom: the breathing waveform (BR), the heartbeat waveform (HB) -in blue- and the ECG -in red-, and the HRV extracted from the radar signal -in blue- and from the ECG -in red-.

#### IV. CONCLUSIONS

A portable and low-cost millimeter-wave radar for short range applications is engineered. Movements in the order of micrometers were successfully characterised in structural and vital signs monitoring. The low-cost feature of the designed radar node allows the development of a radar network.

#### ACKNOWLEDGEMENTS

This work was supported by the Spanish Ministry of Science and Innovation under projects

PID2020-113979RB-C21 and PID2020-113979RB-C22 (MCIN/AEI/10.13039/501100011033). The work of I. Sardinero-Meirás was supported by a pre-doctoral Contract PRE2021-099967 from the Ministry of Science and Innovation. The work of E. Antolinos and Ignacio E. López-Delgado was supported by an FPU Fellowship granted by the Spanish Ministry of Education (FPU18/01525 and FPU20/06405, respectively). The authors would like also to thank Mercé V. Electromedicina [15] for providing the Task Force Monitor to perform the measurements.

#### REFERENCES

- [1] M.G. Amin. *Radar for indoor monitoring: detection, classification and assessment*. CRC Press, 2018.
- [2] W. A. Ahmad and X. Yi, *How Will Radar Be Integrated into Daily life?: mm-Wave Architectures for Modern Daily Life Applications*. IEEE Microwave Magazine, vol. 23, no.5, pp 30-43, 2022
- [3] D.V. Rodrigues and C. Li, *A review on low-cost microwave Doppler radar systems for structural health monitoring*. Sensors , 21(8), pp. 2612,(Mar 2021). MDPI.
- [4] Li, Changzhi and Peng, Zhengyu and Huang, Tien-Yu and Fan, Tenglong and Wang, Fu-Kang and Horng, Tzyy-Sheng and Muñoz-Ferreras, José-María and Gómez-García, Roberto and Ran, Lixin and Lin, Jenshan
- [5] *Radar Evaluation Kits for Various Front Ends*, Mar 2023. [Online]. Available: <https://siliconradar.com/evalkits>
- [6] *120 GHz wide band transceiver - TRA\_120\_045*. Mar 2023. [Online]. Available: [https://siliconradar.com/products/single-product/20ghz-wide-band-transceiver-tra\\_120\\_045/](https://siliconradar.com/products/single-product/20ghz-wide-band-transceiver-tra_120_045/)
- [7] *STM32WBA52*, Mar 2023. [Online]. Available: <https://www.st.com/resource/en/datasheet/stm32wba52cg.pdf>
- [8] *Ultra Low Phase Noise VCXO*, Mar 2023. [Online]. Available: <https://abracon.com/Oscillators/ABLNO.pdf>
- [9] E. Antolinos, F. García-Rial, C. Hernández, D. Montesano, J. I. Godino-Llorente and J. Grajal, *Cardiopulmonary Activity Monitoring Using Millimeter Wave Radars*, Remote Sensing, vol. 12, no. 14, p2265, 2020
- [10] *STM32WBA52*, Mar 2023. [Online]. Available: <https://www.st.com/resource/en/datasheet/stm32wba52cg.pdf>
- [11] A. Broquetas, A. Aguasca, A. Martínez and R. Tomás, *Structural Health Monitoring with 94 GHz radar*, in IGARSS 2018 - 2018 IEEE International Geoscience and Remote Sensing Symposium, 2018, pp.7982-7985.
- [12] S. M. Kay, *Fundamentals of statistical signal processing: estimation theory*. Prentice- Hall, Inc. 1993.
- [13] E. Antolinos and J. Grajal, *Comprehensive Comparison of Continuous-Wave and Linear-Frequency-Modulated Continuous-Wave Radars for Short-Range Vital Sign Monitoring*. IEEE Transactions on Biomedical Circuits and Systems, pp. 1-17, 2023.
- [14] I. E. López-Delgado, E. Antolinos, I. Sardinero-Meirás, M. Gómez Bracamonte, J. D. Arias-Londoño E. Luque-Buzo, F. Grandas, J. I. Godino-Llorente and J. Grajal, *mm-Wave wireless radar network for early detection of Parkinson's Disease by gait analysis*, 2023 IEEE Radar Conference.
- [15] *Mercé V. Electromedicina*, Mar 2023. [Online]. Available: <https://mercev.com/>